Detection of traffic incidents using nonlinear time series analysis

A. D. Fragkou,[1] T. E. Karakasidis,[1,a)] and E. Nathanail[2]
[1]*Laboratory of Hydromechanics and Environmental Engineering, Department of Civil Engineering, University of Thessaly, 38334 Volos, Greece*
[2]*Traffic, Transportation and Logistics Laboratory, Department of Civil Engineering, University of Thessaly, 38334 Volos, Greece*

(Received 5 February 2018; accepted 18 May 2018; published online 6 June 2018)

In this study, we present results of the application of nonlinear time series analysis on traffic data for incident detection. More specifically, we analyze daily volume records of Attica Tollway (Greece) collected from sensors located at various locations. The analysis was performed using the Recurrence Plot (RP) and Recurrence Quantification Analysis (RQA) method of the volume data of the lane closest to the median. The results show that it is possible to identify, through the abrupt change of the dynamics of the system revealed by RPs and RQA, the occurrence of incidents on the freeway and differentiate from recurrent traffic congestion. The proposed methodology could be of interest for big data traffic analysis. *Published by AIP Publishing.*
https://doi.org/10.1063/1.5024924

Incident detection is an important issue for traffic management especially on freeways since it can save time and money as well as contribute to the reduction of carbon emissions. Modern systems of traffic management include traffic cameras and sensors measuring the traffic volume in real time. The ability to analyze the corresponding time series of traffic data and detect incidents on the freeway and differentiate from recurrent traffic congestion is of particular importance. Non-linear analysis and especially methods that are based on phase space reconstructions have proved particularly adapted for detection of changes in the system dynamics. Recurrence plots (RPs) are a method based on phase space reconstruction that can be used to detect different regions of system behavior. In the present study, it is successfully employed for detection of non-recurrent congestion related to incidents such as accidents.

I. INTRODUCTION

Road congestion has been of particular interest to transportation researchers in the last decades. According to the latest report on urban congestion by the Texas Transportation Institute (TTI), in 2014, Americans had to consume in urban trips an extra 6.9 billion hours (i.e., 6.9×10^9 h) and use an extra 3.1×10^9 gallons of fuel, translated into a congestion cost of US $160 billion. For the important destinations, travelers had to allow 48 min to make a trip that takes 20 min in light traffic on an urban freeway (Texas A&M Transportation Institute and INRIX, 2015). In another report, the congestion cost in Europe is estimated to be more than 110 billion Euros, on a yearly basis (European Commission, 2011).

Incident Management (IM) is one of the main activities of Traffic Management Centers (TMCs), since incidents contribute significantly to highway congestion. Such incidents are non-recurrent events that occur at random time and location, are of different types, and usually cause traffic disturbances. Example of incidents is accidents and other traffic disturbances such as debris on the pavement and stalled vehicles on the roadway owing to flat tires or mechanical problems (Zografos *et al.*, 1993). An effective IM system results in reduced duration of traffic incidents and their impact to congestion while it improves the safety of road users, reduces crash victims, and facilitates emergency responders to react efficiently when their intervention is required (Federal Highway Administration, 2010a, 2010b). Incident detection and verification are of critical importance to the incident duration and when efficiently practiced, they enable traffic flow to recover as safely and quickly as possible (Mustafa and Nathanail, 1999; Federal Highway Administration, 2008; and Nathanail *et al.*, 2017).

Many studies have been performed concerning incident detection (Hojati *et al.*, 2014), determination of the spatial relation in terms of distance between the incident locations (Keskin *et al.*, 2011), methods for detecting traffic incidents from probe-car data (Kinoshita *et al.*, 2015), traffic control systems (Ahmed and Hawas, 2015), traffic monitoring to perform real time incident detection (Baiocchi *et al.*, 2015) and methods to assess on underlying statistical properties of short-term traffic volume data (Vlahogianni *et al.*, 2006). Several studies (Martin *et al.*, 2001; Parkany and Xie, 2005; Mahmassani and Liu, 1999; and Prevedouros *et al.*, 2006) provide a synoptic review of incident detection algorithm categories.

In the present study, we investigate the applicability of the Recurrence Plots (RPs) methods for the analysis of system dynamics and the detection of system state modification. The method of RP (Eckmann *et al.*, 1987 and Marwan, 2003) and its quantification (Recurrence Quantification Analysis - RQA) (Zbilut and Webber, 1992 and Marwan *et al.*, 2007) have many applications in Economics and Finance (Addo *et al.*, 2013; Fabretti and Ausloos, 2005; and

a)Email: thkarak@uth.gr

Strozzi *et al.*, 2002), physics (Sparavigna, 2008), Chemistry (Cazares-Ibanez *et al.*, 2005), engineering (Karakasidis *et al.*, 2007; Vlahogianni *et al.*, 2006; Karakasidis *et al.*, 2009; and Wang, 2012), biology (Webber and Zbilut, 1994; Zbilut *et al.*, 2004; Marwan *et al.*, 2002; and Giuliani *et al.*, 2002), patterns of climate change (Zhao *et al.*, 2011), and airborne pollutants (Aceves-Fernandez *et al.*, 2011), just to mention a few. In order to detect transitions of a system, the method of RP was extended by considering epoqs by separating the recurrence plots in smaller windows and applying RQA on each time window (Marwan, 2003 and Facchini *et al.*, 2007). With the aid of epoqs, RQA identifies recurrent phenomena, such us the orbit of the Moon (Facchini *et al.*, 2007).

In this paper, we study time series of the traffic volumes measured on a Greek highway, the Attica Tollway. Measurements were analyzed using the RP and RQA methods in order to investigate the feasibility of incident detection. Some studies in the field exist with use of RPs; however, they focus on the effect of weather conditions on traffic (Vlahogianni and Karlaftis, 2012) as well as on the determination of nonlinearities and stationarity (Vlahogianni *et al.*, 2006). In the present paper, we employ RPs and analyze the results using RQA method in combination with additional criteria, to detect possible incidents and differentiate them from usual traffic congestion. The time series data originated from sensors located on the roadway are described in Sec. II.

II. DESCRIPTION OF THE DATA

Attica Tollway (AT) is an urban freeway of about 70 km, which constitutes the ring road of the greater Greek metropolitan area of Athens. The freeway is a separated facility and each direction consists of 373.6 lane-km. The operator (Attikes Diadromes S.A.), among all others, focuses on providing rapid detection and clearance of incidents. Patrols are supervised by the freeway's Traffic Management Centre (TMC). In-field Intelligent Transport Systems (ITS) equipment includes color closed circuit television (CCTV) cameras, closely spaced emergency roadside telephones, variable message signs, lane control signals, and variable speed limit signs. The 10 km central urban section of AT exhibits the worst traffic conditions along the freeway, with an annual average daily traffic (AADT) of 52 000 vehicles/direction in 2014. Peak hour volume of a typical working day in 2014 was approximately 5300 veh/hr/dir. An average of 20 000 to 25 000 incidents are recorded by TMC per year (Prevedouros *et al.*, 2008 and Attica Tollway website).

Traffic measurements are made by vehicle detection sensors placed on the lanes along Attica Tollway. Each sensor counts every 20 s the volume, speed, and occupancy. Thus, there are 4320 measurements per sensor during a day (24 h) from 00:00 to 24:00. For the present analysis, raw data were used from the sensors, which detected incidents that caused significant length of queues. For the analysis, we performed data normalization and each time series was normalized to zero mean and standard deviation of one ($Y = \frac{x-\bar{x}}{\sigma}$). According to this, from here and below the units of "volume" refer to "normalized volume." Two incidents were identified, one on each direction of travel on the lanes adjacent to the median. Thus, data from the respective sensors were used for the present analysis. Table I shows the positions of the incidents, the time stamp of incident occurrence and termination, the time stamp of queue creation and dissipation, and the queue length as recorded by at the TMC of AT. The graphical representation of the location of the sensors and the incidents is depicted in Fig. 1. From the analysis of the data, it is concluded that an incident is detected by the closest upstream to the incident sensor, which captures the impact on traffic flow, thus the accumulated vehicle queue and related measurements (reduced speed, increased density) which formulate following the incident occurrence (Nathanail and Zografos, 1995). Therefore, for the incident detected at location A28.5 (incident S1), data were analyzed from the upstream sensor 3555, located at A28.00; for the incident S2, located at E28.6, sensor's 3548 (E28.7) data were used (Fig. 1).

According to Table I and from the time series measurements, the starting time of the S1 incident is 12:35, which corresponds to the record t = 2268 of the time series and the starting point of the incident S2 is 8:48, which corresponds to the record t = 1587 of the time series. We must mention that the first record of the time series corresponds to time 00:00. Representative selected time series appear in Figs. 2 and 3.

III. METHODOLOGY AND COMPUTATIONAL DETAILS

A. Recurrence plots (RPs)

Recurrence plot (RP) is a graphical tool introduced by Eckmann *et al.* (1987) in order to extract qualitative

TABLE I. Incident data and associated sensor locations.

Incident code number	Incident position	Date	Incident start time (timeseries point)	Queue start time (timeseries point)	Incident end time (timeseries point)	Queue end time (timeseries point)	Queue's maximum length (meters)	Sensor position	Sensor ID
S1	A 28.5	01/03/2010	12:35 (2268)	12:38 (2277)	13:19 (2402)	13:12 (2381)	2600	VDS A 28.00	3555
								VDS A 28.70	3557
								VDS A 29.30	3604
								VDS A 29.60	3605
S2	E 28.6	02/03/2010	8:48 (1587)	8:51 (1596)	9:27 (1706)	10:45 (1940)	7000	VDS E 27.80	3545
								VDS E 28.30	3547
								VDS E 28.70	3548
								VDS E 29.20	3600

VDS = Vehicle Detecting System

FIG. 1. Schematic view of sensors and incidents on Attica Tollway with their positions.

characteristics of a time series. It is based on the reconstruction of the underlying system phase space. First, we embed the time series $x(t)$ in an m-dimensional space by forming a sequence of vectors

$$\vec{x}_i = \left[x\left(t_i - (m-1)\tau_d\right), x\left(t_i - (m-2)\tau_d\right), \ldots, x(t_i)\right], \quad (1)$$

where τ_d denotes an appropriately selected time delay (Kantz and Schreiber, 2004 and Kennel *et al.*, 1992).

Then, we calculate the distance $d_{ij} = \left|\vec{x}_i - \vec{x}_j\right|$ between points i, j in the m-dimensional reconstructed phase space. Distances are calculated using the Euclidean norm. As a result, a N × N matrix of distances, d_{ij}, is obtained, with N being the number of reconstructed state vectors. Once the distance matrix is calculated, a two-dimensional plot can be created by darkening the pixel located at (i,j), if the distance between points i and j is lower than a given cut-off value ε

$$R_{i,j}(\varepsilon) = \Theta\left(\varepsilon - \|\vec{x}_i - \vec{x}_j\|\right), \quad i,j = 1,\ldots,N, \quad (2)$$

where N is the number of points $\vec{x}_i$ and $\Theta(\|.\|)$ is the Heaviside function.

The Recurrence Plot is symmetric and has a darkened main diagonal corresponding to the identity line. The darkened points forming lines parallel to the main diagonal and their distribution mark the recurrences of the dynamical process.

If the underlying time series is random and possesses no structure, the distribution on the RP will be homogeneous thus resulting in no particular visual patterns. If there is any determinism in the system that generates the time series, the corresponding RP will be characterized by some distinct

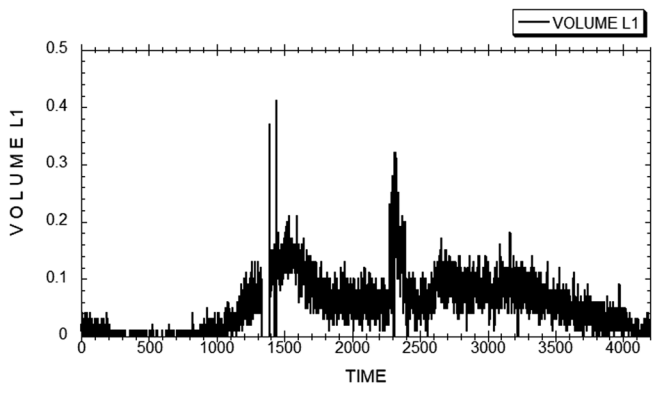

FIG. 2. Time series of volume of vehicles (Lane 1) passing over sensor 3555 (in units of 20 s), from 00:00 to 24:00 on the day of incident S1.

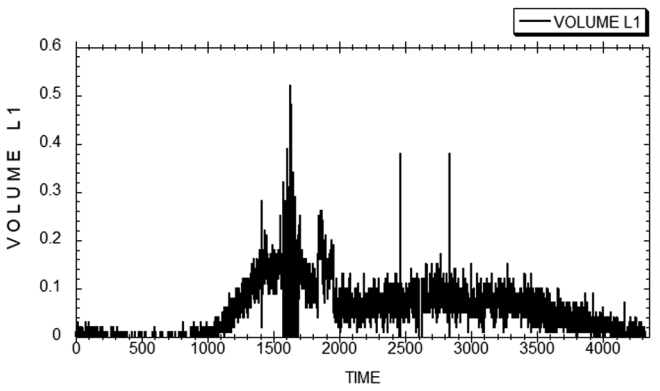

FIG. 3. Time series of volume of vehicles (Lane 1) passing over sensor 3548 (in units of 20 s), from 00:00 to 24:00 on the day of incident S2.

distribution of the points on the plot. RPs exhibit large scale and small scale structure and different conclusions can be reached from examination at different scales (see, for example, Marwan, 2003).

The large scale structure can give the following indications: Homogeneous RPs represent stationary and autonomous systems for which relaxation times are short in comparison with the time spanned by the RP. Such RPs may occur for random time series. Periodic systems result in RPs with diagonally oriented, periodic recurrent structures such as diagonal lines or checkerboard structures. Systems with slowly varying parameters result in a RP characterized by a drift.

Abrupt changes in the dynamics as well as extreme events result in white areas or bands in the RP. The texture (small scale structure) which may consist of single dots, diagonal vertical, or horizontal lines is also indicative of distinct system behavior: Single, isolated recurrence points can occur if states are rare, if they do not persist for any time, or if they present important fluctuations. However, they are not a unique sign of chance or noise. A diagonal line occurs when a segment of the trajectory runs parallel to another segment, i.e., the trajectory visits the same region of the phase space at different times. A vertical/horizontal line marks a time length in which a state does not change or changes very slowly. RPs are symmetrical by construction to the main diagonal. So from the global inspection of an RP, we can have single isolated points (homogeneous RP), diagonal lines (the trajectory visits the same region of the phase space at different times and we may have a deterministic process), horizontal, or vertical lines which they form clusters (the state is "trapped" for some time), and white bands (abrupt changes in system dynamics). Those changes make the system dynamics to come over phase transitions. By covering the RP with sliding windows along the main diagonal and by making RQA on each window as a separate RP, we can find system phase transitions and locate on those abrupt changes.

B. Recurrence quantification analysis (RQA)

Although RPs are a powerful visual tool, they are just a qualitative tool in order to obtain insight about the dynamical system. Webber and Zbilut (1994) extended this idea and defined a number of measurable quantities that can be

extracted from the recurrence plots giving rise to Recurrence Quantification Analysis (RQA). It contains parameters that measure the points on a Recurrence Plot that forming lines (diagonal and horizontal). Among other useful information, someone can extract from this analysis; those parameters can help someone to trace possible changes in the dynamics of a system. One of those parameters is the Recurrence Rate (RR) which counts the number of recurrent points (points below a cut off radius ε) marked with black point on the RP (density of the recurrent points). Recurrence (frequently referred also as %REC) gives the ratio of the number of recurrent points (pixels) to the total number of points (pixels) of the plot

$$\%REC = \frac{1}{N^2}\sum_{i,j=1}^{N} R_{i,j} \quad R_{i,j} = \begin{cases} 1 & (i,j) \text{ recurrent,} \\ 0 & \text{otherwise.} \end{cases} \tag{3}$$

It corresponds to the definition of the correlation sum (Grassberger and Procaccia, 1983).

The RQA can be performed over a sliding time window and in the results plotted as a function of the time window (RQA with epoqs).

The "strength" of the dynamic change can be found by calculating differences between maximum and minimum values of Recurrence Rate. Consider Recurrence Rate as a function of time RR(t) defined in the space D, we say that this function presents local maximum at $t_0 \in D$, when a $\delta > 0$ exist, such as $RR(t) \leq RR(t_0), \forall t \in D \cap (x_0 - \delta, x_0 + \delta)$. Point t_0 called position or time point of local maximum and the value of $RR(t_0)$ is the local maximum. Similarly, function RR(t) presents local minimum at $t_0 \in D$, when a $\delta > 0$ exist, such as $RR(t) \geq RR(t_0), \forall t \in D \cap (x_0 - \delta, x_0 + \delta)$. Point t_0 called position or time point of local minimum and the value of $RR(t_0)$ is the local minimum. So, the biggest the difference between maximum and minimum points, the "strongest" the dynamical change.

C. RP and RQA implementation

For the analysis with the RP method, we use the CRP Toolbox for Matlab, (Marwan, 2008) and for finding the proper embedding and delays on each time series we use the TISEAN toolbox (Hegger *et al.*, 1999) Each time series was embedded in the m-dimensional phase space with the False Nearest Neighbors method (FNN) (Abarbanel, 1996) after finding the proper delay τ using the method of Average Mutual Information (AMI). For the proper embedding, we use the criterion of below 10% falseness of nearest neighbors (Abarbanel, 1996) and for the time delay we use the criterion of the first minimum of the Average Mutual Information (Fraser and Swinney, 1986). After applying those methods

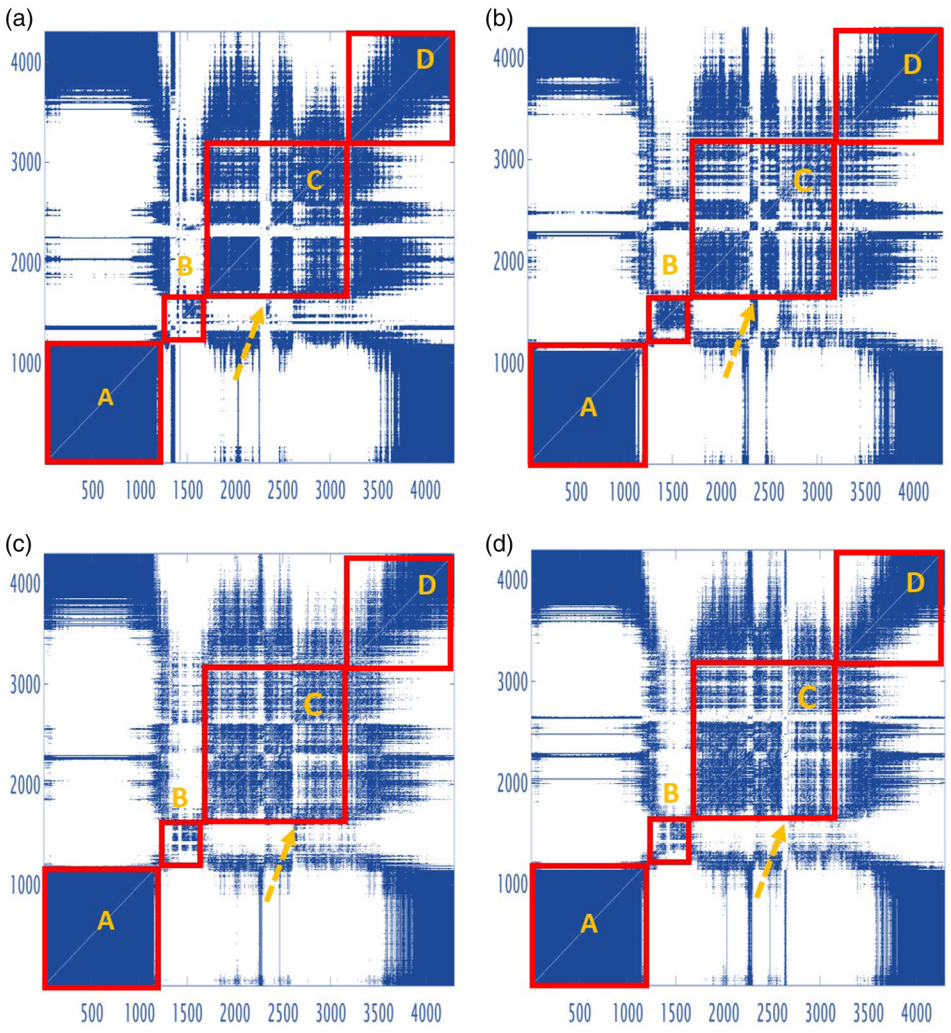

FIG. 4. Recurrence plot of sensors (a) 3555, (b) 3557, (c) 3604, and (d) 3605.

on the time series, we found the proper embedding dimension 9 and delays varied from 1 to 3. Then, Recurrence Plots from each time series were built.

We got useful conclusions from the view of the plots but the RQA leads us to more detailed results and conclusions about tracing incidents. So, we separate the RP at smaller RPs along the diagonal called epoqs which are sliding windows along the main diagonal of the RP. We analyze them with RQA. Each epoq consists of 180 points long (corresponding to 1 h). Successive epoqs are obtained by sliding by one point at a time, resulting a total of 4140 epoqs. We focused on RR parameter which counts the recurrent points on an RP. Big values of the RR parameter denote more recurrent points and the dynamics of the system evolves with no significant changes.

An abrupt change in the dynamics causes white bands on the RP (no recurrent points in this area), so the value of RR parameter falls down to a minimum value. In that case, we have a sudden "drop down" of values from maximum to minimum of the Recurrence rate parameter. The bigger the "drop down," the more abrupt the change in the dynamics caused by a powerful change.

During the day, there are various alternations from maximum to minimum RR values. We calculate the differences between maximum and minimum RR values at the time when a "drop down" was observed. Looking at these differences, we localized the biggest difference and we found that at that time point, it is the exact time when an incident happened and changed the dynamics of the system.

The main purpose of our study is to identify possible incidents using the nonlinear method of RP with epoqs and the RQA with epoqs. We first focus on studying the dynamics of the system by taking a global view of the RP. We saw along the main diagonal different structures. There are regions containing big number of recurrent points forming diagonal and horizontal structure with big lines parallel to the main diagonal and regions which contain small number of recurrent points with no or small lines parallel to the main diagonal. In those regions, we focused on white areas or bands, which are indicative of abrupt changes in dynamics.

For better understanding, we applied further the RQA with epoqs, to find phase transitions and we achieve to separate those times of the day when those abrupt changes are very obvious and affect traffic flow. Considering RR as a function of time, we extract the minimum and the maximum values and we calculate the differences between those two values at a certain time t. The biggest the difference, the more powerful the change of the system dynamics. The strength of those abrupt dynamic changes gives us results, which lead us to detect the incident that occurred and disrupted the normal traffic flow.

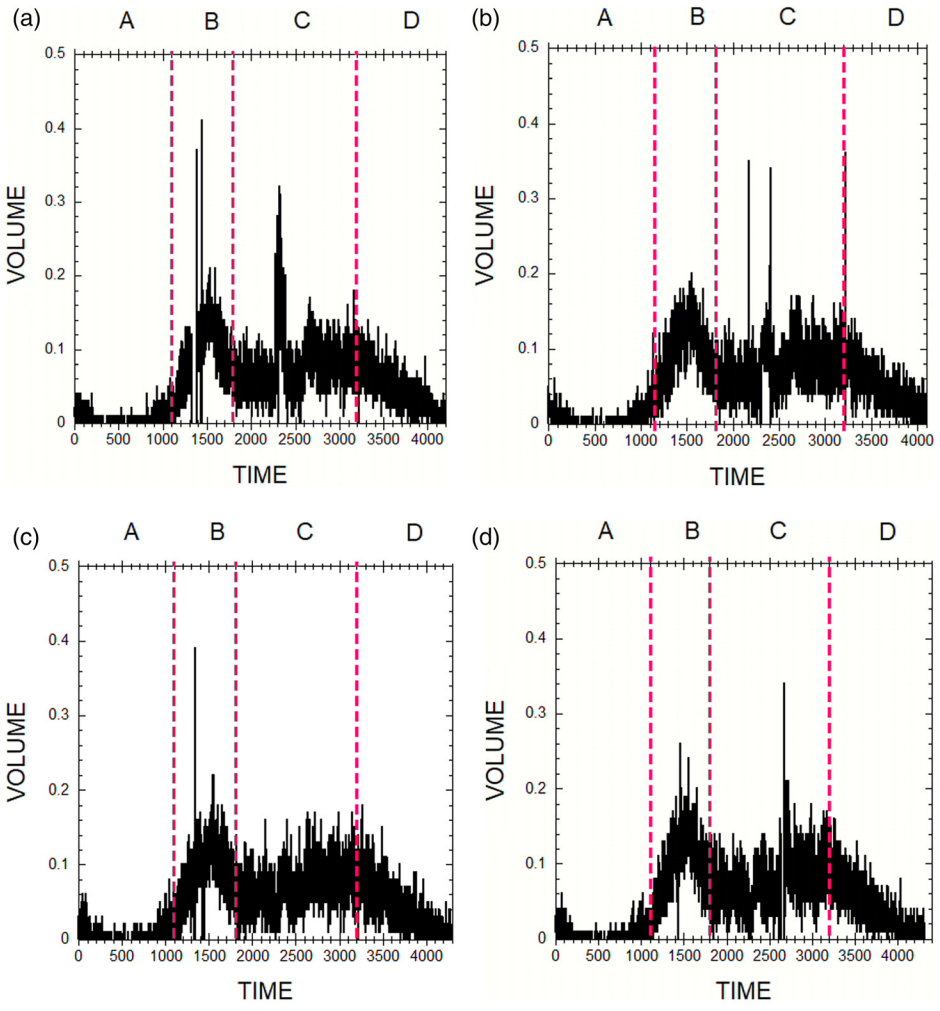

FIG. 5. Time series of sensors (a) 3555, (b) 3557, (c) 3604, and (d) 3605.

IV. RESULTS

A. Incident S1

We calculated the RPs for the time series of the four sensors corresponding to incident S1 (see Table I) and the results are presented in Fig. 4. In a first place, we perform a global visual inspection of the RPs. We can observe in Fig. 4 regions where points on the RPs are very dense, forming black areas. This pattern indicates the existence of a large number of recurrent points forming vertical and diagonal lines, a sign which characterizes regions with significant deterministic behavior. In contrast to these regions, one can also observe other regions where no lines or small lines parallel to the diagonal appear. Such patterns correspond to rather chaotic regions. Moreover, we can observe large white regions, which correspond to abrupt changes of the dynamics of the system.

With a more focused view, we separate the above patterns along the main diagonal regions and in order to be more specific we marked them with red rectangular in A (1–1100), B (1100–1800), C (1800–3200), and D (3200–4350), which correspond to time intervals A(00:00:00–06:06:20) early morning hours, B(06:06:40–09:59:00) the rush hour, C(09:59:20 –17:46:20) middle day hours, D(17:46:40–24:00:00) noon, and late at night hours. Regions A (1–1100) and D (3200–4350) contain large amount of recurrent points forming big deterministic lines, which give us the sign that during those time periods the traffic flow over the sensors was relatively homogeneous and the corresponding volumes do not show any significant fluctuations.

The texture of RPs at regions B (1100–1800) and C (1800–3200) is different. They contain patterns with small diagonal lines and vertical white lines indicators of chaotic behavior with abrupt changes in the dynamics of the system. It is interesting that in sensors 3555 [Fig. 4(a)] and 3557 [Fig. 4(b)], a vertical white line can clearly be distinguished at $t = 2250$ (yellow dashed arrow), denoting that an incident causes an abrupt change in the system behavior. This can be observed also in sensors 3604 [Fig. 4(c)] and 3605 [Fig. 4(d)] at $t = 2550$ (yellow dashed arrow).

Based on the observations of the RPs, the corresponding time series (Fig. 5) can be separated in the corresponding regions A (1–1100) morning hours, B (1100–1800) the rush hour, C (1800–3200) middle day hours, and D (3200–4350) night hours. As we can see in Fig. 5, region A is characterized by small volume values which range from 0 to 0.05. The main characteristic of the B region is the abrupt increase in values up to 0.2 (at point 1500) (which, in fact, corresponds to the peak of rush hour 08:19:40). Next, there is an abrupt decrease from 0.2 to 0.1 (at point 1800) when the rush hour finishes.

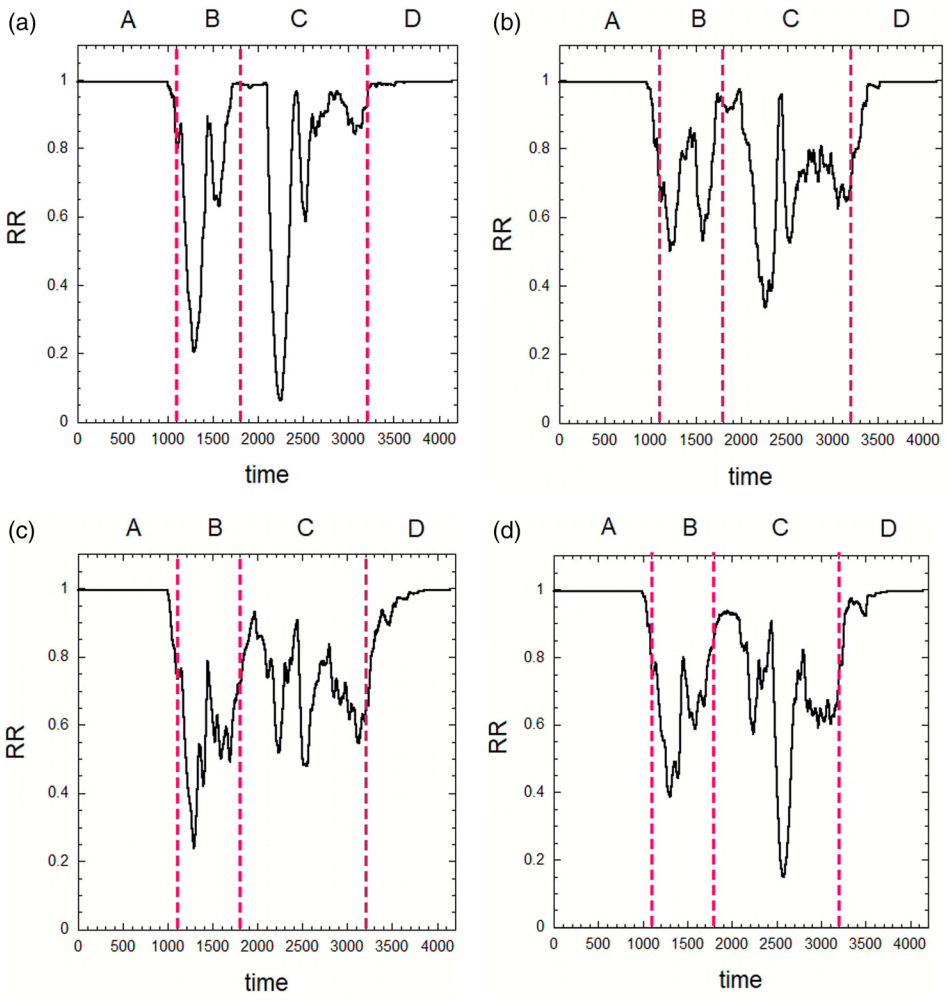

FIG. 6. Recurrence quantification analysis with epoqs (Recurrence Rate) of sensors (a) 3555, (b) 3557, (c) 3604, and (d) 3605.

Volume fluctuations can be observed in the next region C. The main characteristic of this region is that, at the neighborhood of point 2249 (time 12:29:40), we can see an abrupt decrease in traffic volume, as depicted in the timeseries, which coincides with the actual time when the incident was observed and reported by the AT operator. The recorded values of the timeseries are at the range of 0.02 to 0.05. As it is expected, the incident causes traffic disturbance, so during this time, traffic flow is lower and less vehicles pass through the site of the incident. At about point 2380 (time 13:13:20), an abrupt volume increase is observed in the timeseries, and values range from 0.09 to 0.32. This is approximately the time that is reported by the operator of AT as time when the incident's clearance took place and the queue dissipated. Therefore, it is expected that the queued vehicles are released at a higher flow rate than the actual demand. In the last region D, values slowly decrease, which is an indication that as night falls (night hours), the traffic becomes sparser. We must remind the reader that according to Table I the starting time of incident is 12:35 which corresponds to record (2268) of the time series that is close to the point 2250 mentioned above.

In order to have a better understanding of RP observations, we proceed to the quantification of the RPs by applying the extended method of RQA with epoqs (epoq analysis). We construct epoqs of 180 successive records each with time shift of 1 (4140 overlapping windows). Each epoq corresponds to 1 h. We focus on the results of Recurrence Rate. By observing the diagrams of RR in Fig. 6, we see that in regions A and D, it has high values, almost 0.98 nearly all along those regions, meaning that during morning and night hours volume fluctuation is smooth, without problems and possible incidents that may disturb traffic conditions and system dynamics. In regions B and C, the behavior of RR diagrams is different, the main characteristic of these two regions being the alternation of maximum and minimum values of RR parameter (max – min alternations), which gives the differences between maximum and minimum values. Specifically, in region B, we observe three max – min alternations of sensor 3555 [Fig. 6(a)], four max – min alternations of sensor 3557 [Fig. 6(b)], six max – min alternations of sensor 3604 [Fig. 6(c)], and five max – min alternations of sensor 3605 [Fig. 6(d)] with minimum values ranging from 0.2 to 0.55. In region C, we observe nine max – min alternations of sensor 3555 [Fig. 6(a)], eight max – min alternations of sensor 3557 [Fig. 6(b)], eight max – min alternations of sensor 3604 [Fig. 6(c)], and nine max – min alternations of sensor 3605 [Fig. 6(d)] with minimum values ranging from 0.05 to 0.6.

This behavior of RR is consistent with the behavior of the volume time series. With a more analytical view of the four RR diagrams (Fig. 6), we see that at region B (the rush hour) traffic volume changes fast. It increases (point 1200 to 1500 of the timeseries) and then it decreases (point 1500 to 1800). This fast change affects the dynamics of the system and this appears on the diagrams of RR with the above

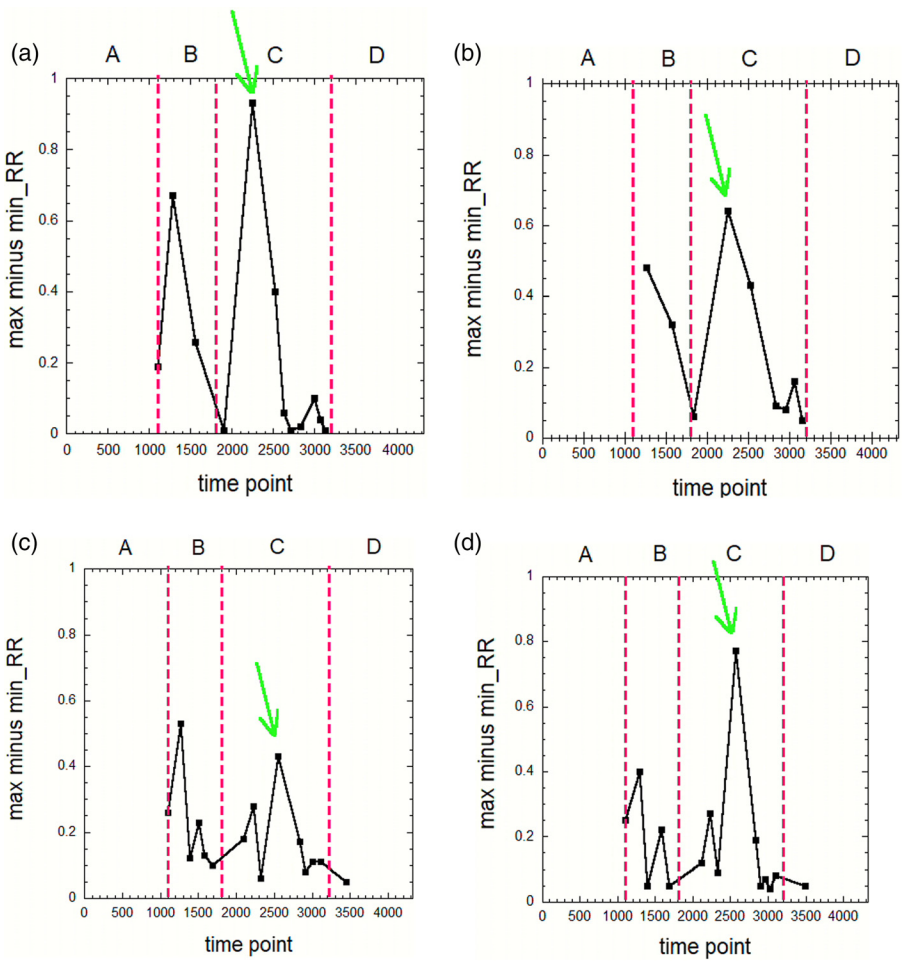

FIG. 7. Points (x axis) of differences between maximum values and minimum values of sensors (a) 3555, (b) 3557, (c) 3604, and (d) 3605.

TABLE II. Time point t of S1 incident detection by each sensor.

Incident S1	Position A28.5, time point t = 2268 (time 12:35:40)			
Sensor	3555	3557	3604	3605
Sensor position	A28.00	A28.70	A29.30	A29.60
Upstream (B)/downstream (A) the incident	B	A	A	A
t time point of incident detection	2240 (time 12:26:20)	2251 (time 12:30:00	2543 (time 14:07:20)	2566 (time 14:15:00)

max – min alternations. Almost, the same behavior is at region C (middle day hours), where those min – max alternations give us the smallest minimum 0.05 at time point 2244 of sensor 3555. This kind of behavior makes someone wonder why this big change happened during the middle day hours having in mind the everyday normal traffic conditions during these hours. So, an abrupt change of the volume means that something happened on the traffic stream and changed abruptly the system dynamics.

Provided that a significant dynamical change in systems dynamics results in a significant decrease in the value of RR parameter, we detect time points where RR has high values (local maximum) and time points where RR has small values (local minimum). In order to detect big and abrupt dynamical changes, we calculate the difference between maximum and minimum values, denoting that at the time point x of the minimum is when the sudden change happened (Fig. 7). Regions A and D do not show such kind of differences, because during those regions the values of RR were stable (0.98).

Focusing on region's B and C differences, we can see that the biggest difference (green arrow) between maximum and minimum values appears at point t = 2251 (time 12:30:00) of sensor 3557 [Fig. 7(b)], which is the nearest downstream sensor to the incident, and t = 2240 of sensor 3555 [Fig. 7(a)], which is the upstream sensor. Based on the available data, this is the exact time of the incident occurrence, according to the results of the method. The other two sensors provide biggest difference at t = 2543 (time 14:07:20) of sensor 3604 [Fig. 7(c)] and at t = 2566 (time 14:15:00) of sensor 3605 [Fig. 7(d)], which are further to the incident site, which means that they impose a time delay to locate any abrupt change. We remind here the reader that according to Table I, the start time of the incident is 12:35 which corresponds to record (2268) of the time series, while

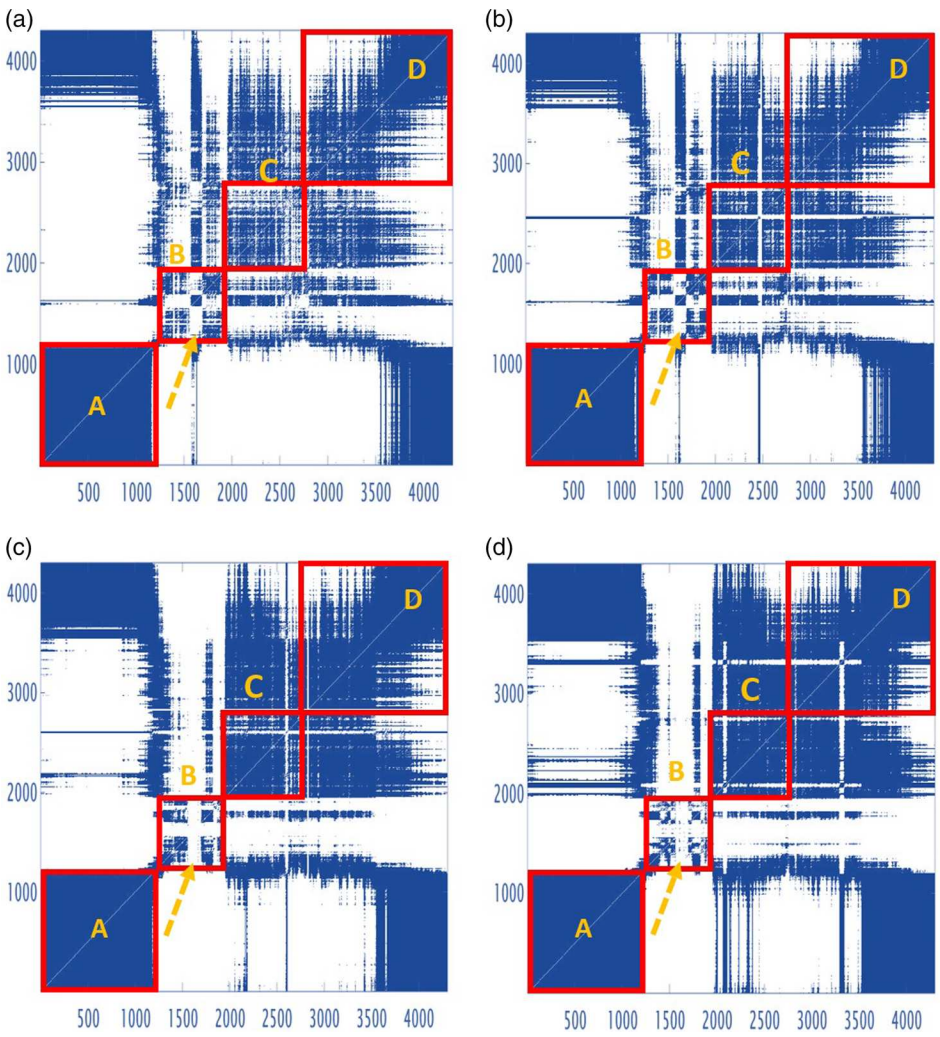

FIG. 8. Recurrence plot of sensors (a) 3545, (b) 3547, (c) 3548, and (d) 3600.

the end time is 13:19, which corresponds to record x = 2402 of the time series.

So, incidents that may disturb the normal traffic flow insomuch as to change the dynamics of the system can be detected by the extended method of RQA with epoqs from all sensors, which are placed in the vicinity of the incident in combination with RPs. Moreover, the method of RQA proved reliable enough to discriminate traffic congestion, which takes place during the rush hour, from incidents, which disturb the normal traffic flow (biggest max – min difference).

We must bear in mind that the difference of time for the different sensors has to do with their distance from the incident location. As we can see in Table II, sensor 3555 is located upstream the incident, while the other sensors are located downstream, thus resulting larger times for the incident detection, since the incident effect propagates backwards.

B. Incident S2

Incident S2 occurred at E 28.6 position on AT and we studied the volume time series of the surrounding sensors (see Table I). From a global inspection of the corresponding RPs (Fig. 8), we can distinguish regions with almost the same texture as in the case of incident S1. So the two regions with very dense points, forming black areas are in the red rectangular regions A (1–1100) (00:00:00–06:06:20) early morning hours, D (2750–4350) (15:16:20–24:00:00) noon, and night hours. In those areas, there is large number of recurrent points forming lines vertical and diagonal which are a characteristic of high deterministic regions. The two other regions are placed in the red rectangular regions B (1100–1900) (06:06:40–10:33:00) the rush hour and C (1900–2750) (10:33:00–15:16:20) middle day hours, where we can observe different kinds of patterns (no lines or small parallel lines). Those kinds of patterns correspond to chaotic regions. Moreover, we can observe white regions, which correspond to abrupt changes of the dynamics of the system.

Specifically, regions A (1–1100) and D (2750–4350) are, as in the case of incident S1, big amounts of recurrent points forming long deterministic lines. As in the case of incident S1, during those time periods, traffic flow is relatively homogeneous and the corresponding volume does not present any significant changes in time.

The texture of RPs at regions B (1100–1900) and C 1900–2750) differs from that of regions A and D. The plots contain patterns with small diagonal lines and vertical white lines indicators of chaotic behavior with abrupt changes in the dynamics of the system. From the view and the size of the white vertical lines especially at region B (1100–1900) in all sensors, it may be concluded that an abrupt change in the dynamics of the system occurs, which could correspond to an incident. Specifically, in sensors 3548 [Fig. 8(c)] and 3600 [Fig. 8(d)], one can distinguish a vertical line near t = 1500 (time 8:19:40) (yellow dashed

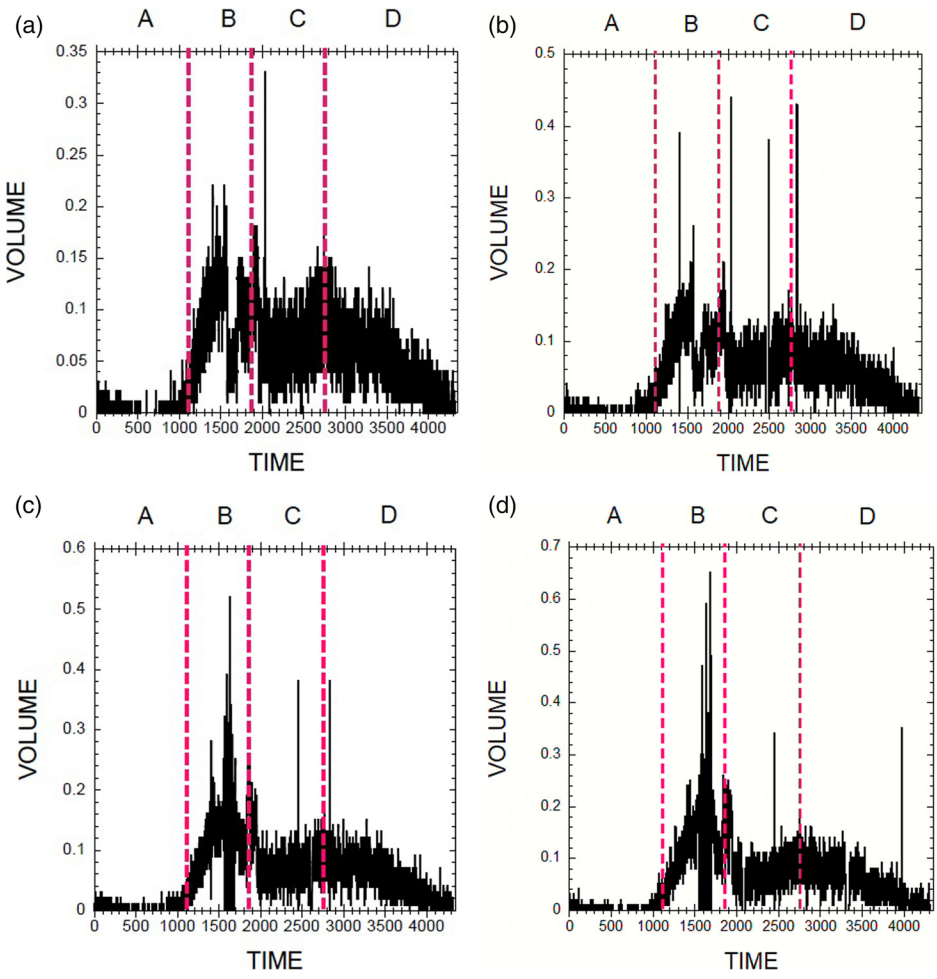

FIG. 9. Time series of sensors (a) 3545, (b) 3547, (c) 3548, and (d) 3600.

arrow). In sensors 3547 [Fig. 8(b)] and 3545 [Fig. 8(a)], the same vertical line can distinguished near t = 1800 (time 10:00:00) (yellow dashed arrow) denoting that an incident makes the system to change abruptly its behavior. We proceed again to the quantification of RPs for more specific results.

Analyzing the time evolution from the time series (Fig. 9), regions A (1–1100) (00:00:00–06:06:20) early morning hours, B (1100–1900) (06:06:40–10:33:00) the rush hour, C (1900–2750) (10:33:00–15:16:20) middle day hours, and D (2750–4350) (15:16:20–24:00:00) noon and night hours can be distinguished. First, small values from 0 to 0.05 are in the A region. Different behaviors can be observed in B region. At the neighborhood of point 1580 (time 8:46:20), the normalized volume values decrease abruptly. As in case of incident S1, the decrease coincides with the incident's occurrence time, as reported by the operator of AT. The values of timeseries range from 0.01 to 0.03. It is the time when traffic is disrupted by the incident and normal traffic flow drops. Furthermore, an abrupt increase is noted around point 1700 (time 9:26:40), which also coincides with the incident's clearance and the volume reaches a value of 0.18. At that time, the traffic resumes with a higher rate that the initial demand, which is owing to the formulated queue. A value ranging from 0.02 to 0.15 can be seen at region C and at region D, where values slowly decrease, an indication that as night falls (night hours) traffic becomes sparser like in the case of incident S1.

Using the RQA, the corresponding diagrams of RR (Fig. 10) are constructed. Looking at regions A and D, RR parameter has high values (almost 0.98), like in the case of incident S1, which denotes that during morning and night hours vehicles move smoothly and the system dynamics are not disturbed.

In regions B and C, the behavior of RR diagrams is changing. Also like in incident S1, the main characteristic of those two regions is the alternation of maximum and minimum values of RR parameter (max – min alternations).

Specifically, in region B, we observe five max – min alternations of sensor 3545 [Fig. 10(a)], five max – min alternations of sensor 3547 [Fig. 10(b)], four max – min alternations of sensor 3548 [Fig. 10(c)], and four max – min alternations of sensor 3600 [Fig. 10(d)] with minimum values ranging from 0.01 to 0.65.

In region C, we observe two max – min alternations of sensor 3548 [Fig. 10(a)], five max – min alternations of sensor 3547 [Fig. 10(b)], three max – min alternations of sensor 3600 [Fig. 10(c)], and five max – min alternations of sensor 3545 [Fig. 10(d)] with minimum values ranging from 0.4 to 0.8.

Focusing on Fig. 10 (RR diagrams), region B (the rush hour) reveals a behavior different than someone expects to be the rush hour. Although the traffic volume changes fast, there is a big max – min alternation. The region C (middle day hours), where two small min – max alternate, defers from the behavior of B region. Such kind of behavior in

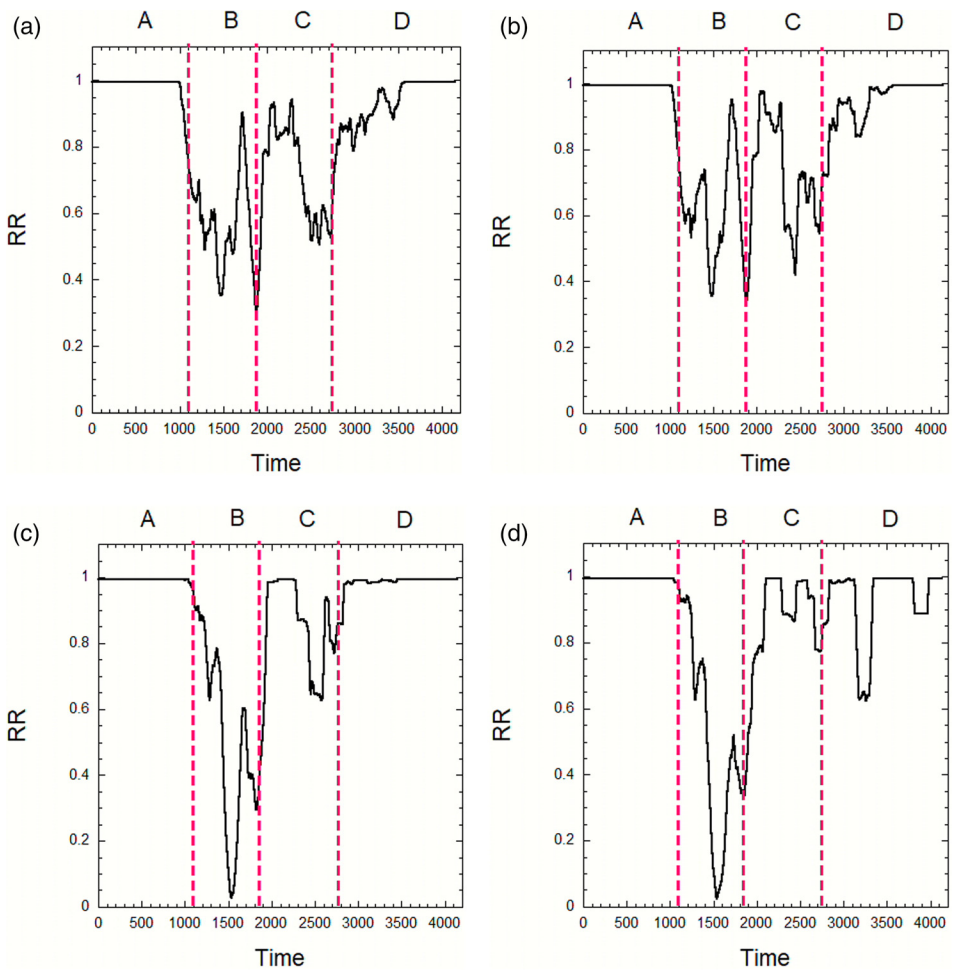

FIG. 10. Recurrence quantification analysis with epoqs (Recurrence Rate) of sensors (a) 3545, (b) 3547, (c) 3548, and (d) 3600.

region B can be attributed to something special like an incident that occurred during the rush hour and the traffic flow changed abruptly its dynamics.

The differences between maximum minus minimum values of the RR parameter (Fig. 11) are bigger in B region than those in C and D regions. Comparing to incident's S1 case, we can see that in region B, although it is the rush hour, a big dynamical change affects the usual traffic flow upon time. B is the region with the biggest difference (green arrows) located at t = 1524 (time 8:27:40) of sensor 3548 [Fig. 11(c)], x = 1536 (time 8:31:40) of sensor 3600 [Fig. 11(d)], and x = 1872 (time 10:23:40) of sensors 3547 [Fig. 11(b)] and 3545 [Fig. 11(a)]. Time points and locations are given in Table III. We remind here that, according to the information provided by TMC (Table III), S2 incident occurred at 8:48 which corresponds to record x = 1587 of the time series. We can see again that sensors detect the event at different times, depending on their positioning (upstream or downstream) and distance from the incident.

Summarizing the results, we can clearly see that if an incident happens during the day along AT, the dynamics of the system changes abruptly. In both incidents, data were analyzed with RPs and RQA and successfully detected the occurrence of the incident in a combined analysis of the sensor time series measurements of the traffic volumes.

Incident S1 which is positioned at A28.5, occurred at 12:35 on 01/03/2010 which corresponds to record x = 2268 in timeseries. From Table II, sensor 3557 which is downstream the incident at A28.70 presents the biggest critical points difference (max-min) at x = 2251. At the same time, sensors 3604 and 3605 located, also, downstream the incident (A29.30 and A29.60, respectively) present the biggest critical points differences (max minus min) at x = 2543 and x = 2566, respectively, meaning that the abrupt change in dynamics affected those sensors with a time delay. Moreover, sensor 3555, located upstream the incident, which was affected by the incident, presents the biggest critical points difference (max minus min) at x = 2240.

A similar behavior is observed for incident S2 which is positioned at E 28.6 and occurred at 8:48 on 02/03/2010, which corresponds to record point x = 1587 in time series. From Table III, sensors 3548 and 3600 which are upstream the incident at E 28.70 and E 29.20 present the largest critical points difference (max-min) of Recurrence Rate at x = 1524 and x = 1536, respectively. Downstream sensors 3545 and 3547 present the largest critical difference (successive max-min) of RR at x = 1872. We also see that for this incident all sensors were affected and with both methods of RP and RQA, we are able to identify those effects.

V. CONCLUSIONS

RP with epoqs is a useful tool to detect dynamic state transitions during the evolution of a dynamical system. In the present study, by applying RP to traffic data, we observe

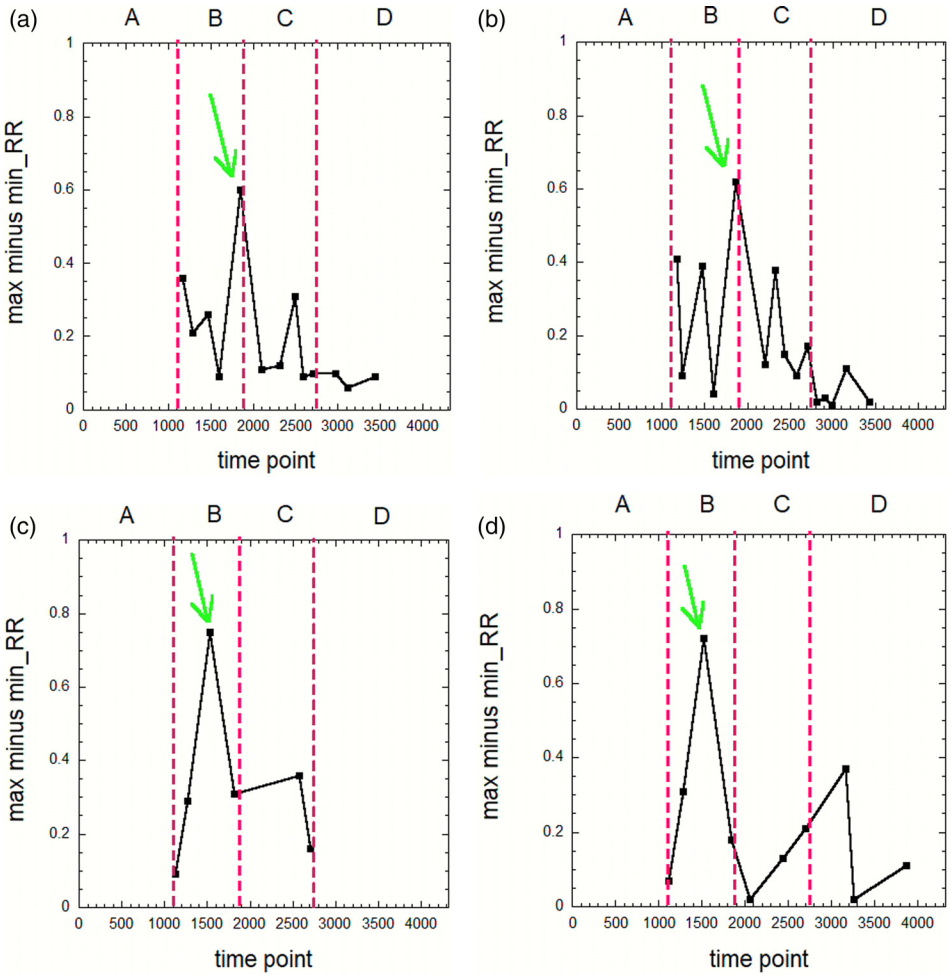

FIG. 11. Points (x axis) of differences between maximum values and minimum values of sensors (a) 3545, (b) 3547, (c) 3548, and (d) 3600.

TABLE III. Time point t of S2 incident detection by each sensor.

S2	Position E28.6, time point t = 1587 (time 8:48:40)			
Sensor	3545	3547	3548	3600
Sensor position	E 27.80	E 28.30	E 28.70	E 29.20
Upstream (B)/downstream (A) the incident	A	A	B	B
t time point of incident detection	1872 (time 10:23:40)	1872 (time 10:23:40)	1524 (time 8:27:40)	1536 (time 8:31:40)

state transitions and understand the dynamics of the system by inspection of the RPs. Big white vertical lines of RP provide the indication of abrupt change in the dynamics and we detect during this time a possible incident that may disturb and change the dynamics of the system.

The quantification of RPs by finding RR gave an extra helping on identifying those abrupt changes in dynamics of the system and empowered our belief that those changes are due to incidents that occurred during the time period of our analysis data. Finding the bigger value of the maximum - minimum alternations between successive values of RR parameters in all regions of every sensor allows us to find the time when the incident occurred and permits us to discriminate it from the recurrent traffic congestion.

RPs and RQA with epoqs proved to be a powerful method for detecting incidents which disturb the normal traffic flow and can comprise an extra tool to new traffic monitoring and management mechanisms of the roadways' Traffic Management Centers.

Abarbanel, H., *Analysis of Observed Chaotic Data* (Springer, Verlag, 1996).

Aceves-Fernandez, M. A., Ramos-Arreguín, J. M., Pedraza-Ortega, J. C., Sotomayor-Olmedo, A., and Tovar-Arriaga, S., "Finding trends of airborne harmful pollutants by using recurrence quantification analysis," Am. J. Environ. Eng. **1**, 10–14 (2011).

Addo, P. M., Billio, M., and Guegan, D., "Nonlinear dynamics and recurrence plots for detecting financial crisis," North Am. J. Econ. Finance **26**, 416–435 (2013).

Ahmed, F. and Hawas, Y. E., "An integrated real-time traffic signal system for transit signal priority, incident detection and congestion management," Transportation Res. Part C: Emerging Technol. **60**, 52–76 (2015).

Baiocchi, A., Cuomo, F., De Felice, M., and Fusco, G., "Vehicular ad-hoc networks sampling protocols for traffic monitoring and incident detection in intelligent transportation systems," Transp. Res. Part C: Emerging Technol. **56**, 177–194 (2015).

Cazares-Ibáñez, E., Vázquez-Coutiño, G. A., and García-Ochoa, E., "Application of recurrence plots as a new tool in the analysis of electrochemical oscillations of copper," J. Electroanal. Chem. **583**, 17–33 (2005).

Eckmann, J. P., Kamphorst, S. O., and Ruelle, D., "Recurrence plots of dynamical systems," Europhys. Lett. **4**, 973 (1987).

European Commission, *White Paper: Roadmap to a Single European Transport Area* – towards *a* Competitive *and* Resource Efficient Transport System, COM 144, Final 2011, Brussels (2011).

Fabretti, A. and Ausloos, M., "Recurrence plot and recurrence quantification analysis techniques for detecting a critical regime. Examples from financial market indices," Int. J. Mod. Phys. C **16**, 671–706 (2005).

Facchini, A., Mocenni, C., Marwan, N., Vicino, A., and Tiezzi, E., "Nonlinear time series analysis of dissolved oxygen in the Orbetello Lagoon (Italy)," Ecol. Modell. **203**, 339–348 (2007).

Federal Highway Administration, "Service patrol handbook," US DOT Report No. FHWAHOP-08-031, 2008, see http://www.ops.fhwa.dot.gov/publications/fhwahop08031/ffsp_handbook.pdf.

Federal Highway Administration, "Traffic incident management handbook updated," US DOT, Office of Travel Management, Washington, DC (2010a).

Federal Highway Administration, "Best practices in traffic incident management," Report No. FHWA-HOP-10-050, 2010b, see http://ops.fhwa.dot.gov/ publications/fhwahop10050/fhwahop10050.pdf.

Fraser, A. M. and Swinney, H. L., "Independent coordinates for strange attractors from mutual information," Phys. Rev. A **33**, 1134 (1986).

Giuliani, A., Benigni, R., Zbilut, J. P., Webber, C. L., Sirabella, P., and Colosimo, A., "Nonlinear signal analysis methods in the elucidation of protein sequence− structure relationships," Chem. Rev. **102**, 1471–1492 (2002).

Grassberger, P. and Procaccia, I., "Measuring the strangeness of strange attractors," Phys. D **9**, 189–208 (1983).

Hegger, R., Kantz, H., and Schreiber, T., "Practical implementation of nonlinear time series methods: The TISEAN package," Chaos **9**, 413 (1999).

Hojati, A. T., Ferreira, L., Washington, S., Charles, P., and Shobeirinejad, A., "Modelling total duration of traffic incidents including incident detection and recovery time," Accid. Anal. Prev. **71**, 296–305 (2014).

Kantz, H. and Schreiber, T., *Nonlinear Time Series Analysis* (Cambridge University Press, 2004), Vol. 7.

Karakasidis, T. E., Fragkou, A., and Liakopoulos, A., "System dynamics revealed by recurrence quantification analysis: Application to molecular dynamics simulations," Phys. Rev. E **76**, 021120 (2007).

Karakasidis, T. E., Liakopoulos, A., Fragkou, A., and Papanicolaou, P., "Recurrence quantification analysis of temperature fluctuations in a horizontal round heated turbulent jet," Int. J. Bifurcation Chaos Appl. Sci. Eng. **19**, 2487–2498 (2009).

Kennel, M. B., Brown, R., and Abarbanel, H. D., "Determining embedding dimension for phase-space reconstruction using a geometrical construction," Phys. Rev. A **45**, 3403 (1992).

Keskin, F., Yenilmez, F., Çolak, M., Yavuzer, I., and Düzgün, H. S., "Analysis of traffic incidents in METU campus," Procedia-Social Behav. Sci. **19**, 61–70 (2011).

Kinoshita, A., Takasu, A., and Adachi, J., "Real-time traffic incident detection using a probabilistic topic model," Inf. Syst. **54**, 169–188 (2015).

Mahmassani, H. and Liu, Y., "Dynamics of commuting decision behavior under advanced traveler information systems," Transp. Res. Part C: Emerging Technol. **7**, 91–107 (1999).

Martin, P. T., Perrin, J., Hansen, B., Kump, R., and Moore, D., "Incident detection algorithm evaluation," Prepared for Utah Department of Transportation (2001).

Marwan, N., "Encounters with neighbors," Ph.D. thesis (University of Potsdam, 2003).

Marwan, N., "Cross recurrence plot toolbox," Reference Manual Version 5.12, Release 25, 2008.

Marwan, N., Romano, M. C., Thiel, M., and Kurths, J., "Recurrence plots for the analysis of complex systems," Phys. Rep. **438**, 237–329 (2007).

Marwan, N., Wessel, N., Meyerfeldt, U., Schirdewan, A., and Kurths, J., "Recurrence-plot-based measures of complexity and their application to heart-rate-variability data," Phys. Rev. E **66**, 026702 (2002).

Mustafa, M. A. and Nathanail, T., "Advanced incident management and tolling enforcement systems based on image processing and video technologies," in *Advanced Video-Based Surveillance Systems* (Springer, US, 1999), pp. 182–191.

Nathanail, E., Kouros, P., and Kopelias, P., "Traffic volume responsive incident detection," in *World Conference on Transport Research* (Elsevier, Shanghai, 2017).

Nathanail, T. G. and Zografos, K. G., "Simulation tool for evaluating effectiveness of freeway incident response operations," Transp. Res. Rec. **1485**, 105–111 (1995).

Parkany, E. and Xie, C., "A complete review of incident detection algorithms & their deployment: What works and what doesn't," NETCR 37, Project No. NETC 00-7, 2005.

Prevedouros, P., Halkias, B., Papandreou, K., and Kopelias, P., "Freeway incidents in the United States, United Kingdom, and Attica Tollway, Greece: Characteristics, available capacity, and models," Transp. Res. Rec.: J. Transp. Res. Board **2047**, 57–65 (2008).

Prevedouros, P., Ji, X., Papandreou, K., Kopelias, P., and Vegiri, V., "Video incident detection tests in freeway tunnels," Transp. Res. Rec.: J. Transp. Res. Board **1959**, 130–139 (2006).

Sparavigna, A., "Recurrence plots of sunspots, solar flux and irradiance," e-print arXiv:0804.1941 (2008).
Strozzi, F., Zaldívar, J. M., and Zbilut, J. P., "Application of nonlinear time series analysis techniques to high-frequency currency exchange data," Phys. A **312**, 520–538 (2002).
Texas A&M Transportation Institute and INRIX, "Urban Mobility Scorecard 2015," August 2015, see http://mobility.tamu.edu/ums/report/.
Vlahogianni, E. I. and Karlaftis, M. G., "Comparing traffic flow time-series under fine and adverse weather conditions using recurrence-based complexity measures," Nonlinear Dyn. **69**, 1949–1963 (2012).
Vlahogianni, E. I., Karlaftis, M. G., and Golias, J. C., "Statistical methods for detecting nonlinearity and non-stationarity in univariate short-term time-series of traffic volume," Transp. Res. Part C: Emerging Technol. **14**, 351–367 (2006).
Wang, C., Zhong, Z., and Jiaqiang, E., "Flow regime recognition in spouted bed based on recurrence plot method," Powder Technol. **219**, 20–28 (2012).
Webber, C. L. and Zbilut, J. P., "Dynamical assessment of physiological systems and states using recurrence plot strategies," J. Appl. Physiol. **76**, 965–973 (1994).
Zbilut, J. P., Giuliani, A., Colosimo, A., Mitchell, J. C., Colafranceschi, M., Marwan, N., and Uversky, V. N., "Charge and hydrophobicity patterning along the sequence predicts the folding mechanism and aggregation of proteins: A computational approach," J. Proteome Res. **3**, 1243–1253 (2004).
Zbilut, J. P. and Webber, C. L., "Embeddings and delays as derived from quantification of recurrence plots," Phys. Lett. A **171**, 199–203 (1992).
Zhao, Z. Q., Li, S. C., Gao, J. B., and Wang, Y. L., "Identifying spatial patterns and dynamics of climate change using recurrence quantification analysis: A case study of Qinghai-Tibet plateau," Int. J. Bifurcation Chaos Appl. Sci. Eng. **21**, 1127–1139 (2011).
Zografos, K. G., Nathanail, T., and Michalopoulos, P., "Analytical framework for minimizing freeway-incident response time," J. Transp. Eng. **119**, 535–549 (1993).